Period-adding bifurcations and chaos in a bubble column

Viviane S. M. Piassi, Alberto Tufaile,[a] and José Carlos Sartorelli
Instituto de Física, Universidade de São Paulo, C. P. 66318, 05315-970 São Paulo, Brazil

(Received 26 September 2003; accepted 9 March 2004; published online 21 May 2004)

We obtained period-adding bifurcations in a bubble formation experiment. Using the air flow rate as the control parameter in this experiment, the bubble emission from the nozzle in a viscous fluid undergoes from single bubbling to a sequence of periodic bifurcations of k to $k+1$ periods, occasionally interspersed with some chaotic regions. Our main assumption is that this period-adding bifurcation in bubble formation depends on flow rate variations in the chamber under the nozzle. This assumption was experimentally tested by placing a tube between the air reservoir and the chamber under the nozzle in the bubble column experiment. By increasing the tube length, more period-adding bifurcations were observed. We associated two main types of bubble growth to the flow rate fluctuations inside the chamber for different bubbling regimes. We also studied the properties of piecewise nonlinear maps obtained from the experimental reconstructed attractors, and we concluded that this experiment is a spatially extended system. © *2004 American Institute of Physics.* [DOI: 10.1063/1.1721112]

Injecting air through a submerged nozzle can form air bubbles in a liquid, and this phenomenon is fundamental in a wide range of two-phase flow equipment. In addition to the field of chemical engineering, the time series analysis from the experiments of bubble columns has many points of contact with the theory of dynamical systems, and it presents some examples of typical routes to chaos, besides attracting the interest of different areas of physical sciences. Depending on the values of the airflow rate and fluid parameters, such as viscosity and surface tension, the bubble formation evolves through a sequence of bifurcations. Once bubbles are formed, each bubble or bubble group rises toward the liquid surface creating bubble trains. In this article we focus attention on dynamic effects produced in a bubble column by inserting tubes of different length in the pneumatic system between the solenoid valve and the chamber under the nozzle. Besides period-doubling and chaos, also observed is a bubbling sequence related to period-adding bifurcations. The mechanism behind the different bubbling types is examined by images obtained of the forming bubbles, as well as from the time interval between bubbles, and comparisons of reconstructed attractors with piecewise maps.

I. INTRODUCTION

Although a bubble as a volume of air formed within a liquid is a common phenomenon, its formation is a nonlinear event that involves the interpenetrability of two fluids in motion relative to each other, with each fluid in a different thermodynamic phase. If a train of bubbles is formed from a nozzle into a liquid, the bubbling dynamics presents a richness of behavior, such as period-doubling, route to chaos via intermittency, and generation of spherical shells of air called antibubbles,[1] just to cite some of them. In addition to this, there are applications in diverse fields, such as petrochemical, bubble chambers, pharmaceutical and ocean physics,[2] which stimulated some authors to study the transition from regular to chaotic behavior in bubble formation.

One way to reveal the dynamical mechanisms underlying bubble formation is to use phenomenological models. The basic mechanism involved in bubble formation from a nozzle into liquids in many models depends on some form of the force balance acting on the bubble. At low flow rates, when a gas is flowing through a submerged nozzle, the surface tension between the two phases acts in order to prevent the gas encroachment inside the liquid, forming an attached bubble. As the bubble grows, the buoyancy and inertial forces overcome the surface tension, and the bubble detaches from the nozzle. Increasing the flow rate new forces are considered. For example, Zhang and Shoji[3] photographed bubble formation and growth to gain some insight into dynamic behavior, reporting a bubbling sequence involving single, double and triple periods. They used an approximated model, in which the dynamics of bubble formation was represented by the sum of all stresses over the forming bubble, such as buoyancy, gas momentum flux, surface tension, added-mass, drag forces and bubble interactions until the break up of the bubble neck. Some authors studied the bubble formation observing the dominating characteristic time scales in order to comprehend the basics of dynamics, for example, studying bubbles from boiling process, Hernández-Cruz *et al.*[4] considered a class of one-dimensional maps and added noise to explain the bubble dynamics, observed from a vertical glass capillary in a pool of water. Comparing experimental data with a combination of two alternating quadratic maps known as combined maps, Tufaile and Sartorelli[1] simulated a discontinuous bifurcation caused by the coalescence of two bubbles. Studies on air bubble formation under sound wave stimuli identified route to chaos via quasi-periodicity, resonant states, period-doubling, and chaos in the same way as

[a]Author to whom correspondence should be addressed. Electronic mail: tufaile@if.usp.br

observed in the two-dimensional circle map dynamics.[5,6] Some studies also report the existence of spatiotemporal chaos based on the instabilities created by mutual interactions between separated bubbles.[7,8]

Nevertheless, there is a bubbling behavior observed by some authors,[9,10] but not classified yet, in which the bubble emission starts from single bubbling, undergoing a sequence of periodic bifurcations of k to $k+1$, occasionally interspersed with some chaotic regions, and returning to single bubbling, as the control parameter increases. Even in everyday situations, such as bubble formation in a glass poured with carbonated beverages,[11] is observed transitions involving single bubbling, bubble pairs, and bubble triplets emerging from a single nucleation site during the degasification process. The present study seeks to analyze this aspect of this period-adding phenomenon. Our main assumption is that the period-adding bifurcation in bubble formation depends on flow rate variations in the chamber under the nozzle. This assumption can be experimentally tested by placing a tube between a gas reservoir and the chamber under the nozzle in a bubble column experiment. Using a viscous liquid, we can focus on the dynamic of bubble formation without the effects of bubble deformation observed in less viscous liquids like water.

It is worthy of remark that the majority of the dynamical systems found in the literature, which present similar behavior of period-adding bifurcations and chaos, have the main structure based in two parts: a self-exciting system subjected to a periodic force or a some sort of excitation, whereas in our work we have a nonlinear system without any periodic external force. A question about this statement is how to explain these two parts in a bubbling experiment. We can conjecture that this experiment is a spatially extended system consisting of two main parts: the first one is the pneumatic system connected to the second one represented by the two-phase flow.

This paper is organized as follows: the next section presents some aspects of period-adding maps, and some characteristics of the mechanism of creation and destruction of periodic orbits in these maps. In Sec. III, we describe the experiment of a bubble column in a viscous liquid. In Sec. IV, some features of flow rate fluctuations are presented, as well as experimental period-adding bifurcations. The reconstructed attractors obtained from the time between successive bubbles are compared to low-dimensional maps that mimic period-adding bifurcations in Sec. V. Finally, we present the conclusions of our findings in Sec. VI.

II. PERIOD-ADDING SYSTEMS

Period-adding differs from period-doubling scenario by the class of series representation observed in each scenario. In period-doubling scenario there is a sequence of periods represented by a geometrical series, while in period-adding scenario this sequence is represented by an arithmetical series. Period-adding sequence appears in different dynamical systems, and there are some interesting and important examples of systems that exhibit this behavior, typically characterized by a sequence of increasing periodicity occasionally separated by regions of chaos. Huang *et al.*[12] observed period-adding in an optogalvanic circuit, consisting of a neon bulb shone by a modulated green-light He–Ne laser. Ren *et al.*[13] reported period-adding and chaos in the interspike interval series generated by a neural pacemaker inserted in rats. A system that connects biology and physics is the Fitzhugh–Nagumo model for mimicking the firing neurons in nervous systems. This model, which can be implemented by a relaxation circuit,[14] supports period-adding behavior.[15] Many other electronic circuits are known to possess complex behavior oscillatory cycles with multiple periods.[16] In the context of two-phase flow, Elnashaie *et al.*[17,18] proposed a model to explain the bubbling phenomena in a fluidized bed catalytic reactor, in which homoclinic chaos and the period-adding route to complex nonchaotic attractors were observed, which can result in an increase in the production of polyethylene. We identified the period-adding route in the results presented by Simon *et al.*[19] for the dynamics of an acoustically driven air bubble, in which they presented bifurcation diagrams of the phase of the radius and acoustic pressure amplitude. We also found an analogous behavior in the results presented by Nagatani[20] for the studies of the transition through multiply periodic to chaotic motion for a model of shuttle bus displacement.

The examples given before suggest that many aforementioned processes are related to relaxation oscillations, in which sudden transitions are preceded by intervals of quiescence. The most important characteristic of a relaxation oscillator is that there is a jump discontinuity or a sharp derivative in the phase space, enabling us to compare piecewise maps with experimental data in order to gain insight into the problems of ''fast-slow'' systems.[21]

We found in the literature different forms of classification for period-adding systems. LoFaro[21] has found two types of bifurcation by iterating discontinuous maps, in which one type of bifurcation, a period $k+1$ orbit, emerges to coexist with a preexisting period k orbit, and, in the other type, the period k orbit disappears leaving a period $k+1$ orbit. Besides this classification, Holden and Fan,[22] arranged period-adding in three groups. The first group involves dynamics of periodic regions of increasing periodicity interspaced by regions of chaos. The second group is characterized by continuous bifurcations without a chaotic region. In the third group the bifurcation at each period is discontinuous without chaotic dynamics. The first type of period-adding is observed in experiments of a driven series RLD circuit,[23] in which the capacitor of a RLC circuit is replaced by a varactor diode. The second group can be found in the literature in a fluidized bed system.[17,18] In many driven oscillating systems characterized by a relatively slow storage of energy followed by a rapid release of this energy, the period-adding bifurcations of the third group can be represented by a piecewise mapping $f(x_n)$ (see Refs. 21 and 24). The following map exemplifies the third group:

$$x_{n+1}=\begin{cases}\mu+0.7x_n, & \text{if } x_n<0.5,\\ 0.2, & \text{if } x_n\geqslant 0.5,\end{cases} \tag{1}$$

and using the parameter μ we can observe a reverse order period-adding route, with the gap between each straight line

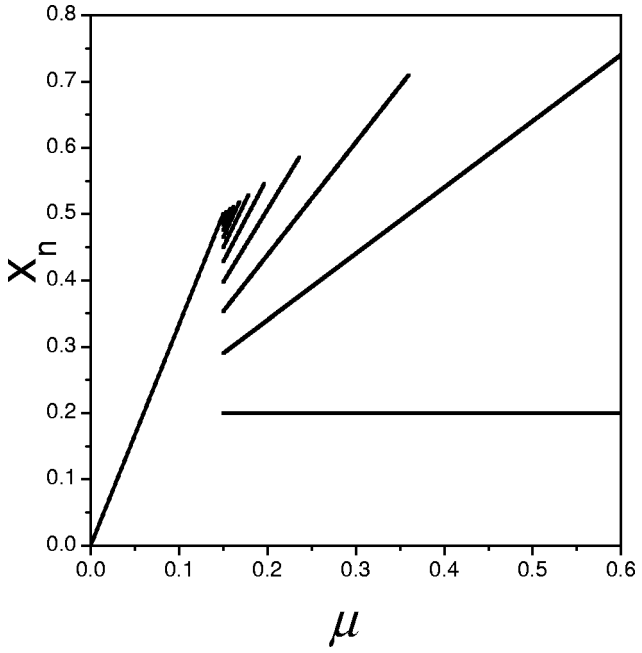

FIG. 1. Period-adding bifurcation scenario for the piecewise linear map of Eq. (1).

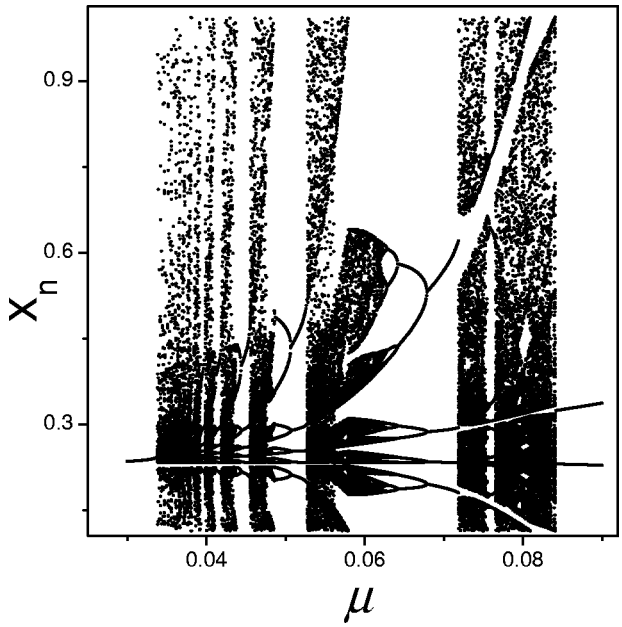

FIG. 2. A bifurcation diagram for the cubic map [Eq. (3)] showing period-adding route and chaos. We can observe periodic orbits, such as period 4 ($\mu=0.07$), period 5 ($\mu=0.051$), period 6 ($\mu=0.045$), and period 7 ($\mu=0.041$), separated by regions of chaos obtained by period-doubling route. The coefficients of cubic function are $a1=119.0$, $b1=-73.0$, $c1=14.1$, and $d1=-0.56$. The straight line coefficients are $a2=-0.1703$ and $b2=0.286\,48$.

of this map controlled by this parameter. Figure 1 shows the respective period-adding bifurcation diagram. Examples in literature can be found in Ref. 24 that deduced some features of piecewise linear maps with horizontal segments. Avrutin and Schanz[25] studied some scaling properties of similar systems.

As we increase the control parameter μ, the map stays at a period 1 orbit until the variable x reaches the discontinuity, and an inverse cascade of $k+1$ bifurcations occurs. The period 1 exists while the left branch of the map intersects the identity function. Thus as we shift the control parameter, the transition from period 1 to period-adding scenario is given by the introduction of a gap between the two different parts of the map, creating a reinjection mechanism due to a channel between the left side of $f(x_n)$ and the identity function. The horizontal segment right after the discontinuity makes any value coming from the left side of the map shrink to the point 0.2. Thus, it is possible to determine each value of parameter μ_m where the bifurcation from period k to period $k+1$ occurs by

$$\mu_m = 0.5 - 0.7 f^m_{k\to k+1}(0.2), \tag{2}$$

where $k=m+2$. The solution with period 2 takes place for all values of μ higher than μ_0. Using this expression, we have obtained the value of $\mu_0=0.36$. On the other hand, the limit case of $m=\infty$ was obtained considering the last value of period 1 before the discontinuity $f^{\infty}(0.2)=0.5$, which gives $\mu_\infty=0.15$.

The previous example shows some features of the transition from a continuous system to a discontinuous one exhibiting period-adding bifurcations, observed in the third group. However, we can also construct maps that present period-adding characteristics of the first group interspaced by period-doubling and chaos, combining properties of a cubic function $f(x)$, and a straight line $g(x)$ with a gap between them, for example,

$$x_{n+1}=\begin{cases} f(x_n)=a_1(x_n-\mu)^3-b_1(x_n-\mu)^2 & \\ \qquad +c_1(x_n-\mu)+d_1, & \text{if } f(x_n)<1, \\ g(x_n)=a_2x_n+b_2, & \text{if } f(x_n)\geqslant 1, \end{cases} \tag{3}$$

where μ is the control parameter, and a_1, b_1, c_1, d_1, a_2, and b_2 are the coefficients of the piecewise map. Despite the low-dimensional phase space of this map, it is able to show a large variety of complex dynamical regimes. A numerical example of the bifurcation structures is given in Fig. 2. The phenomenon of period-adding is preserved, although with the appearance of some new characteristics, for example, the period 1 orbit at the beginning of the bifurcation diagram, is related to a stable fixed point of a saddle-node bifurcation, different from the case of piece-linear map where there is only one fixed point. Arising from this bifurcation, a series of chaotic windows followed by period halving cascades lead finally to a period 2 orbit. In Sec. V we compare some attractors of this map with experimental data.

III. EXPERIMENTAL APPARATUS

The bubble column consists of a cylindrical tube with an inner diameter of 11 cm and 70 cm in height. The bubbles are issued by injecting air through a metallic nozzle submerged in a viscous fluid (20% water/80% glycerol), and the liquid is maintained at a level of 15 cm, as shown in Fig. 3. The nozzle with an inner diameter of 0.78 mm and length of

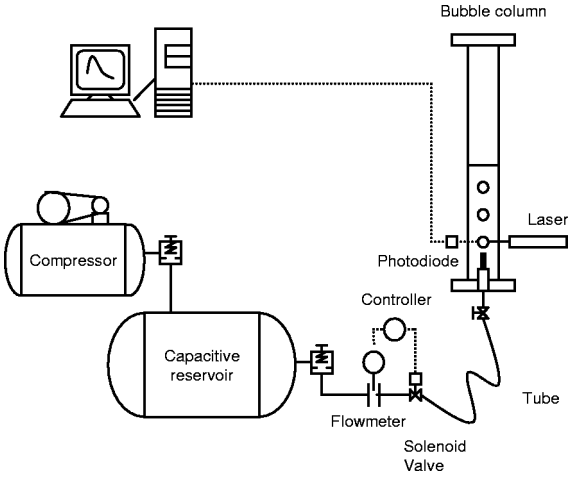

FIG. 3. Schematic diagram of the experimental apparatus.

3.8 cm is placed with its tip 6.5 cm below the liquid surface to avoid wall effects on the forming bubble. The nozzle is attached to a chamber with a capacity of 30 ml. Air from a compressor is injected to a capacitive reservoir, and a proportionating solenoid valve (Aalborg PSV-5) controlled by a PID controller (BTC-220) sets the air flow to the chamber under the nozzle. The flow rate is measured by a flowmeter Aalborg (GFM47). The pressure drop across the solenoid valve is around 15 psi for the working range of air flow rate. In order to study the influence of the pneumatic system in the bubble formation dynamics, a tube is connected from the solenoid valve to the chamber under the nozzle, keeping fixed the influence of other elements of the pneumatic system. The tube inner diameter is 4.1 mm, and we used four different tube lengths: the shortest tube is 10.5 cm long (tube A) to minimize the pneumatic resistance, 50.0 cm (tube B), 138.5 cm (tube C) and 261.0 cm long (tube D). Using a ramp function of the controller, the air flow rate ranged from 80 to 140 ml/min. There is a ball valve located beneath the nozzle for maintenance purpose.

The detection system is based on a laser-photodiode system,[4,5] with a horizontal He–Ne laser beam focused in photodiode placed 2 mm above the nozzle. The time interval between successive bubbles is measured by a time circuitry inserted in a PC slot, with a time resolution equal to 1 μs. The input signals are voltage pulses induced in a resistor and defined by the beginning (ending) of scattering of a laser beam. The pulse width is the time interval t_n (n is the bubble number), and the time delay between two pulses defines the crossing time (dt_n) of a bubble through the laser beam, so that the total time interval is $T_n = t_n + dt_n$. Series of time intervals between bubbles $\{T_n\}$ were obtained, and then the bubble mean frequency was calculated as $f_b = 1/\langle T \rangle$. We estimated the total experimental noise around 100 μs in the period 1 behavior. We also recorded the bubble formation with a VHS camera in order to obtain their profiles in different bubbling regimes.

IV. EXPERIMENTAL PERIOD-ADDING BIFURCATIONS

The time interval between bubbles was recorded while slowly increasing the air injection rate into liquid, as shown in Figs. 4(a)–4(d), in order to observe the importance of the tube length in the bubbling dynamics. For the shortest tube (tube A), in Fig. 4(a), the bubbling dynamics is a period 1 regime for this range of flow rate. We can observe, in region around 110 ml/min, an inflexion of the experimental curve. In Fig. 4(b), the effect of the tube lengthening (tube B) is shown by a closed looplike sequence called *bifurcation bubble* in the bubbling from 107 to 117 ml/min, close to the same region in which the inflexion was observed in the previous case. Figure 4(c) shows the bifurcation sequence for the tube C, with a period 1 until 93 ml/min, period-doubling

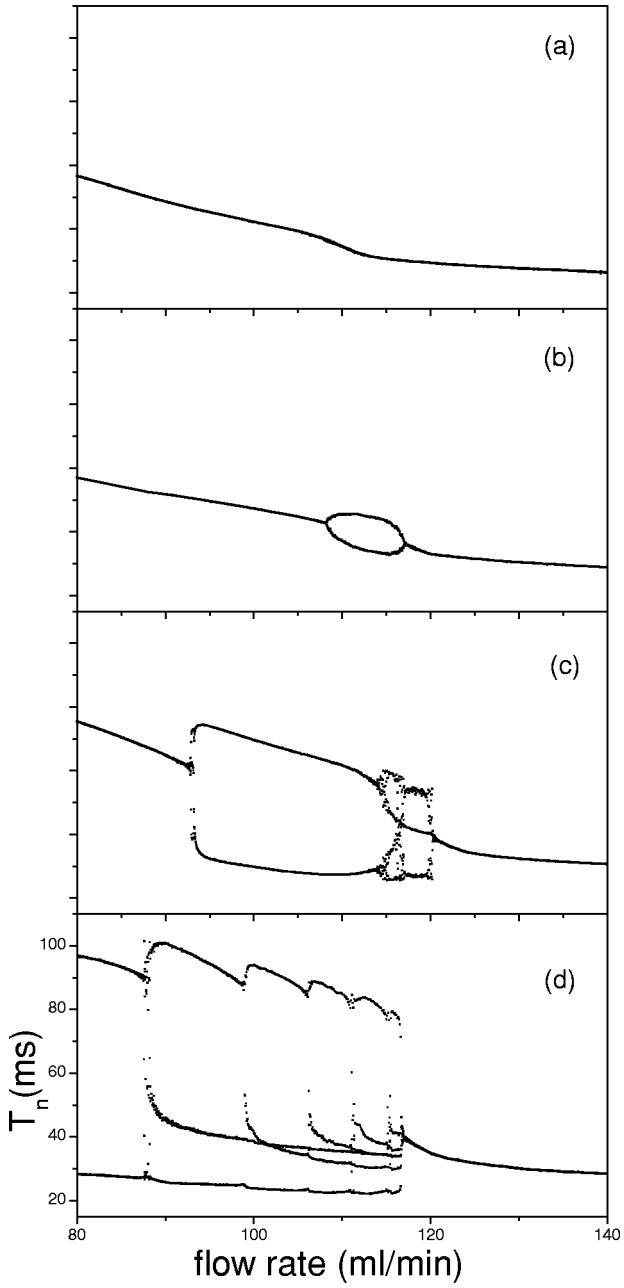

FIG. 4. Experimental bifurcation diagrams with the flow rate as the control parameter. In (a) period 1 is obtained using tube A for the range of air flow rate between 80 and 10 ml/min; in (b) bifurcation bubble using tube B; in (c) bifurcation bubble with period-doubling, chaos, and period 3 using tube C; and (d), using tube D, a sequence of period-adding bifurcations. The intersection between some branches in (d) appears because it is a projection. Each attractor can be completely untangled in two dimensions (see Fig. 11).

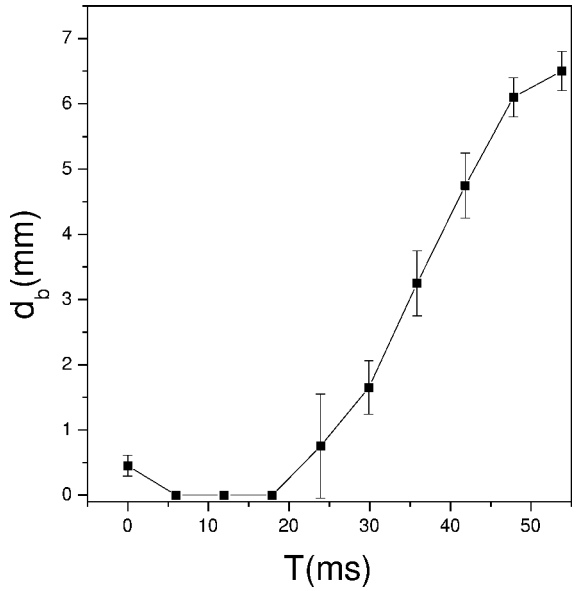

FIG. 5. Evolution of visible bubble diameter as a function of time before the bifurcation bubble at a flow rate of 91 ml/min. There is a bubble retraction for the first 18 ms.

from period 1 to period 2 at 93 ml/min, another period doubling from period 2 to a noisy period 4 at 114 ml/min, a thin region of chaos around 117 ml/min, followed by a period 3 from 117 to 120 ml/min, and after this a period 1, closing the bifurcation bubble. Some reconstructed attractors for this region are discussed at the end of this section (see Fig. 9). The last case, in Fig. 4(d), shows the phenomenon of period increase using the longest tube (tube D). For this case the bifurcation system was in a period 2 up to 88 ml/min, and evolved to periods 3, 4, 5, 6, 7, and 1.

We recorded sequences of events during the bubble formation in order to throw some light on the phenomena for different values of the control parameter. This technique is a complimentary analysis tool for studies of bubble formation dynamics,[26] giving additional information about the bubble shape. We chose the tube B and studied the bubble growth in three regions of Fig. 4(b), before and after the bifurcation bubble, and in a period 2 inside the bifurcation bubble. Figure 5 shows the visible bubble diameter evolution in the period 1, before the bifurcation bubble. When the bubble moves upwards through the detachment position, the gas supply to the bubble is not cut off, which results in the formation of a meniscus linking nozzle and a bubble that lengthens as the bubble rises. This process continues until the meniscus breaks near the tip of the nozzle and the bubble detaches itself. The remaining air snaps back quickly, passes its spherical equilibrium position and performs a retracted motion into the nozzle. The contraction of this small bubble can be observed in Fig. 5 for the first 5 ms, and it represents the liquid pressure overcoming the pressure exerted on the bubble formation by the gas. After the bubble retraction, there is a 12 ms time interval in which no bubble is observed. During this stage, in the same way as the nozzle restricts the air flow, it prevents the liquid from entering the gas chamber. The air chamber takes up to a few milliseconds to pressurize, depending on the air flow rate, and the bubble becomes visible again. Hence, the bubble grows until the detachment, and a new small bubble appears, reinitiating the bubble formation cycle.

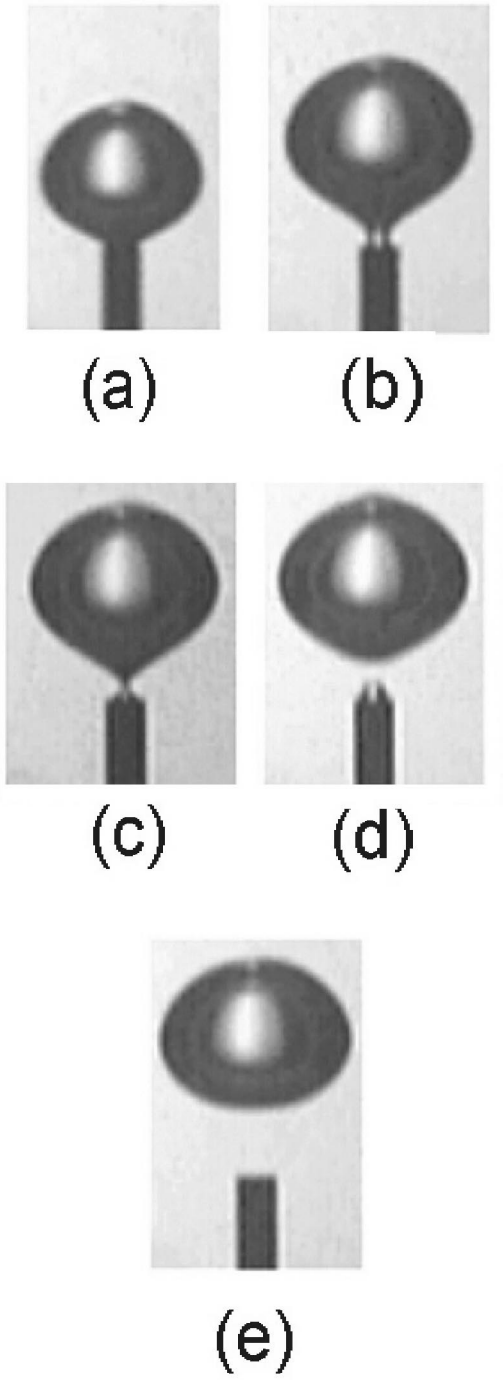

FIG. 6. Images of bubble growth for 91 ml/min. In (a) a bubble grows attached to the nozzle, in (b) bubble lifts off and the neck appears collapsing later in (c). In (d) a small bubble appears and retracts in (e).

Some bubble profiles are shown in Fig. 6. We can observe the meniscus breaking and bubble retraction in these figures of bubble formation, with a similar sequence observed by Davidson and Schuler.[27] In Fig. 6(a) the bubble grows as it is attached to the nozzle, in Fig. 6(b) the bubble lifts off and the neck appears, in Fig. 6(c) the meniscus constricts, in Fig. 6(d) there is a small bubble attached to the

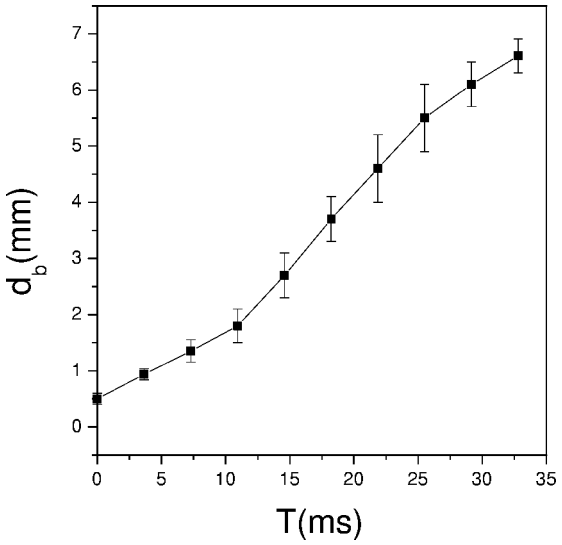

FIG. 7. Evolution of bubble diameter as a function of time at a flow rate of 134 ml/min. As each bubble breaks away from the nozzle it leaves behind a nucleus for the next bubble.

nozzle while the previous bubble emerges, and in Fig. 6(e) the small bubble retracts completely into the nozzle.

Even though after the bifurcation bubble the bubbling returns to a period 1 behavior as seen in Fig. 4(b), for flow rates higher than 117 ml/min, the images of bubble growth present a different evolution in comparison to those of period 1 for the bubbling before the bifurcation bubble. Figure 7 shows the bubble diameter as a function of time, for a flow rate of 134 ml/min, in which bubbles are formed in a period 1 for all tube lengths. As each bubble breaks away from the nozzle, it leaves behind a nucleus for the next bubble. The main difference between this bubble formation process and the previous one is that there is no bubble contraction, and the bubble grows continuously, with the diameter increasing in the same way as observed in the period 1 before the critical flow rate region for a time after 20 ms. In Fig. 8 some bubble profiles for this regime are presented.

For the first case, the bubble contraction relates to flow rate fluctuations, with a ''negative'' flow rate for the extreme cases of weeping through the nozzle into chamber. Thus, the gas flow rate to the bubble varies with time. In the second case the flow rate is high enough to compensate the effects of the tube, with the continuous bubble growth indicating that there is no flow rate fluctuation.

For intermediate conditions, from 107 to 117 ml/min in Fig. 4(b), we observed that period-doubling is an alternation between the two previous cases, with the lower branch of period-doubling related to constant flow rate, and the upper branch of period-doubling related to flow rate fluctuations.

Increasing tube length using the tube C, we obtained period-adding interspaced by period-doubling and chaos between periods 2 and 3. In Fig. 9 are shown the reconstructed attractors for two different flow rate values. In Fig. 9(a) a noisy period 4 is obtained for 115 ml/min, and Fig. 9(b) shows a structured chaotic attractor for a flow rate of 117 ml/min. For these two attractors, besides the alternating bubbling of period 2 of Fig. 4(b), the time between bubbling

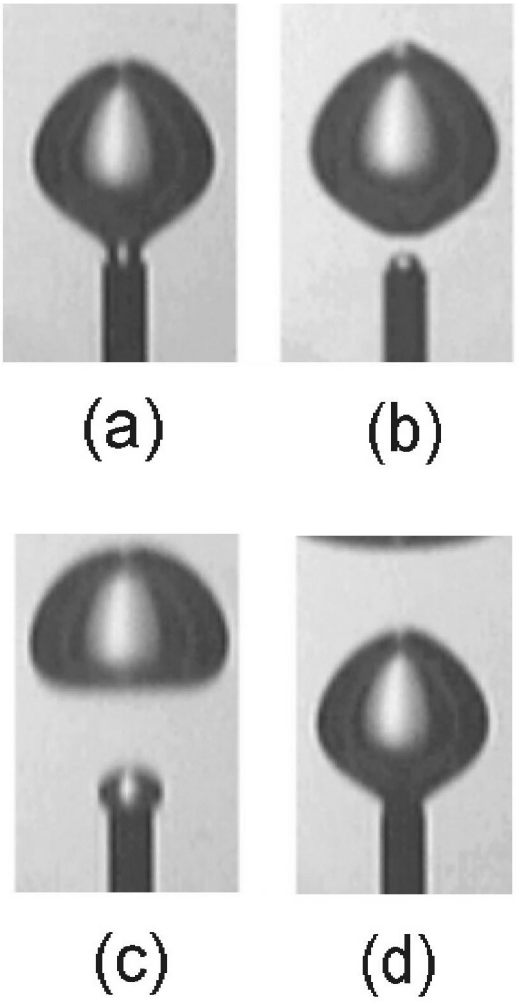

FIG. 8. Bubble profiles at an air flow rate of 134 ml/min. In this situation there is no bubble contraction. In (a) there is a bubble with a neck, after this, in (b), the neck collapses, and in (c) and (d) a small bubble appears and grows continuously.

becomes more complex. The time series of the chaotic attractor has the main characteristics of intermittent systems, with points in laminar phases separated by sporadic points out of sequence around 40 ms, resembling relaminarization process behavior. The attractor of Fig. 9(b) has a sequence of periodic points (period 5), and occasionally some points visiting the whole attractor, and hence possesses unpredictable long-term behavior.

V. STAIRCASE AND COMPARISON BETWEEN RECONSTRUCTED ATTRACTORS

The time series shown in Fig. 4(d) represents a more developed scenario of period-adding than the time series shown in Figs. 4(a)–4(c), with a period sequence 2, 3, 4, 5, 6, 7, ending in a period 1. In order to analyze this bifurcation sequence we obtained the winding number r calculated for each value of flow rate, using the series $\{T_n\} = \{T_1, T_2, \ldots, T_N\}$.[24] The partitions $\{J_n\}$ from this time series were assigned as logic 1 corresponding to values of T_n up to 68 ms, and logic 0 corresponding to time values higher than

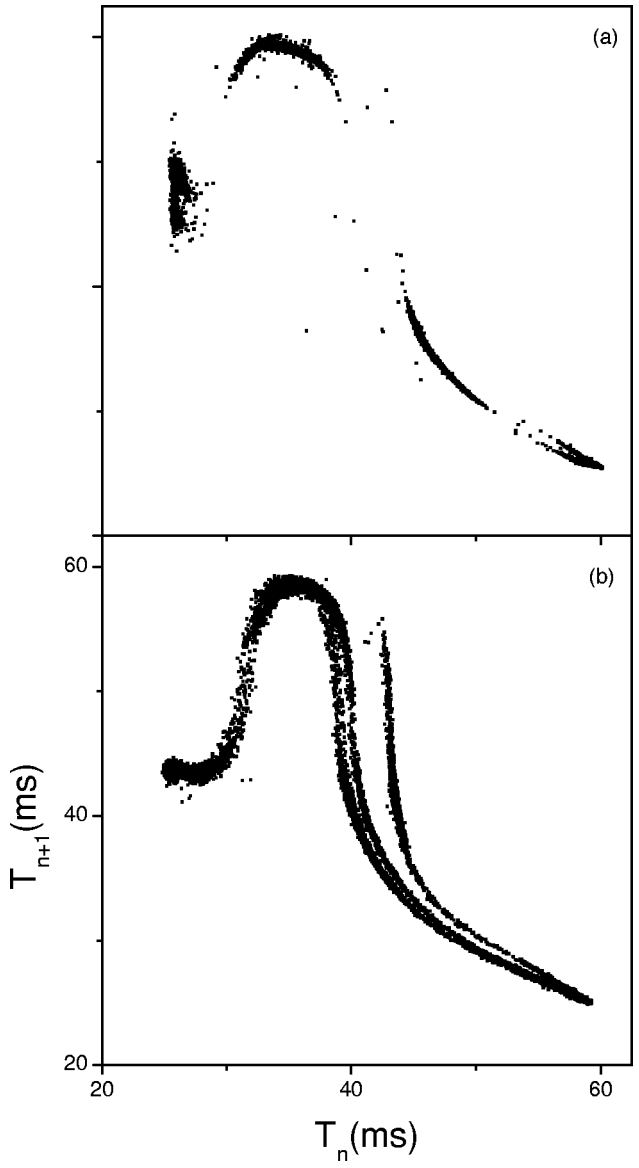

FIG. 9. Time-delay plots for two different flow rates using tube C. In (a) a period 4 and (b) a large structured chaotic attractor.

68 ms, so that we have isolated the bifurcation branch associated with the bubble retraction, with the winding number r as

$$r = \lim_{N \to 50} \frac{\Sigma_{n=1}^{N} J_n}{N}. \tag{4}$$

Figure 10 depicts a staircase obtained for flow rate values from 80 to 140 ml/min from the data of the bifurcation diagram of Fig. 4(d). The periodic windows correspond to some kind of resonant states of the bubbling with plateaus forming a staircase for values of r equal to 1:2, 2:3, 3:4, 5:6, 6:7, and collapsing in the period 1 with winding number 1:1. At the plateau edges there are flow rate values where two plateaus coexist. These regions, where the system stays times in one plateau times in the other, characterize one type of period-adding bifurcation described by LoFaro,[21] in which there are bifurcations from a single period k orbit to the

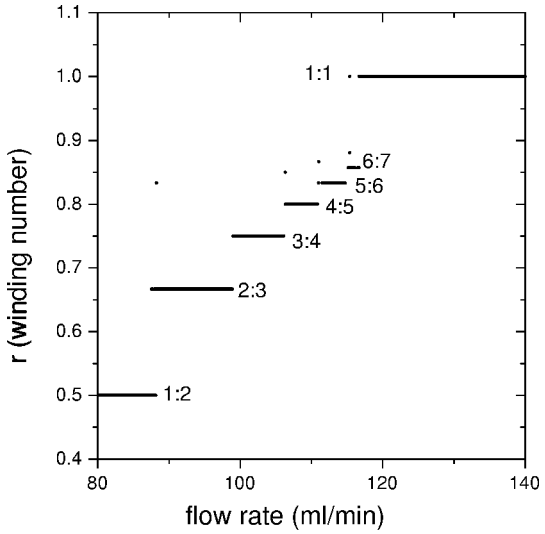

FIG. 10. Staircase obtained with winding number (r) versus flow rate in the period-adding scenario using tube D.

coexistence of a period k with a period $k+1$ orbit, and then to a single period $k+1$ orbit, as the flow rate is increased.

The longest tube (tube D) made possible more states of bubble formation in the condition of continuous flow separated by one state in which the bubble contraction occurred. Using this tube, when we reduced the flow rate under 80 ml/min, the distance of each branch of period 2 increased without the appearance of period 1, until the weeping has caused instabilities in the bubbling due to dripping into the chamber connected to the nozzle.

The periodic attractors obtained for some flow rate values are shown in Fig. 11. In Fig. 11(a), for a flow rate of 83 ml/min, we observed a period 2. In Fig. 11(b) is shown a reconstructed attractor of a period 3 for a flow rate of 90 ml/min. A period 4 is presented in Fig. 11(c) for a flow rate of 102 ml/min. In Fig. 11(d) a period 5 is observed for a 109 ml/min flow rate. Figure 11(e) shows a period 6 obtained for a flow rate of 113 ml/min, and finally for a flow rate of 116 ml/min we can observe a period 7.

Our next step was looking for a simple map that replicates the dynamics of time interval between bubbles from the intriguing attractors of Fig. 11, due to the fact that a map can be directly related to the time series from the experiment. The choice was done based on the idea that the data suggest the existence of an expanding manifold. For example, in Fig. 12 the attractor points reproduce some iterations similar to those observed when a trajectory passes through a corridor formed by the points and first angle bisector $T_{n+1} = T_n$. Although there is a point at (34 ms, 30 ms) indicating that a three-dimensional space unfolds completely the dynamics of the attractor of Fig. 11(f), the main period-adding properties of these attractors embedded in a codimension$=1$ can be explained in a two-dimensional space. Initially, we have tried to fit a parabola to the five points at the left of the bisector of the attractor of Fig. 12, however the family of maps obtained presented mainly the properties of intermittency, making us discard this map. After that, we have used a cubic map introduced in Sec. II. The attractors of Fig. 13 are obtained

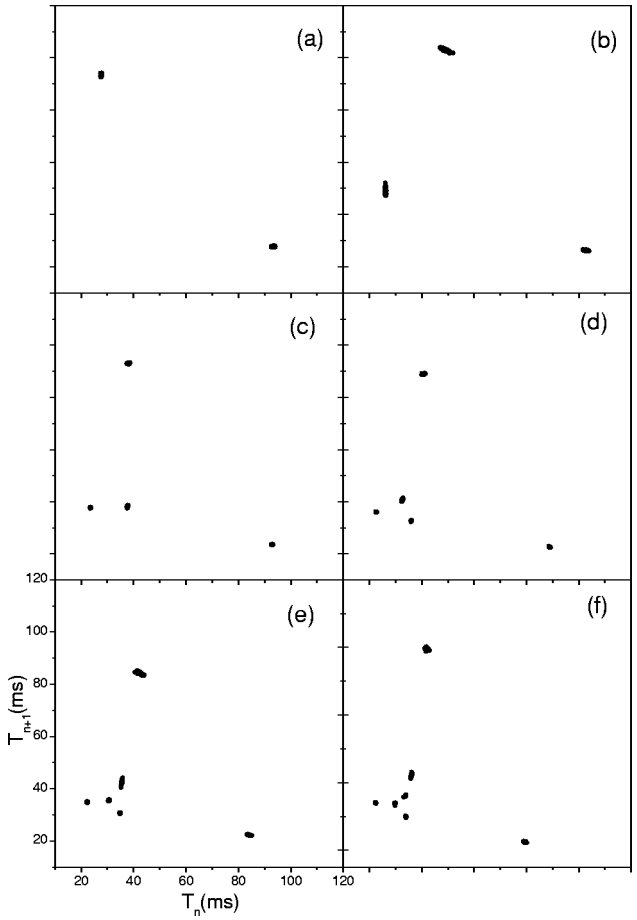

FIG. 11. Reconstructed attractors from the experiment using tube D, for the flow rates in (a) 83 ml/min with a period 2, (b) 90 ml/min with period 3, (c) 102 ml/min with period 4, (d) 109 ml/min with period 5, (e) 113 ml/min with a period 6, and (f) 116 ml/min with period 7.

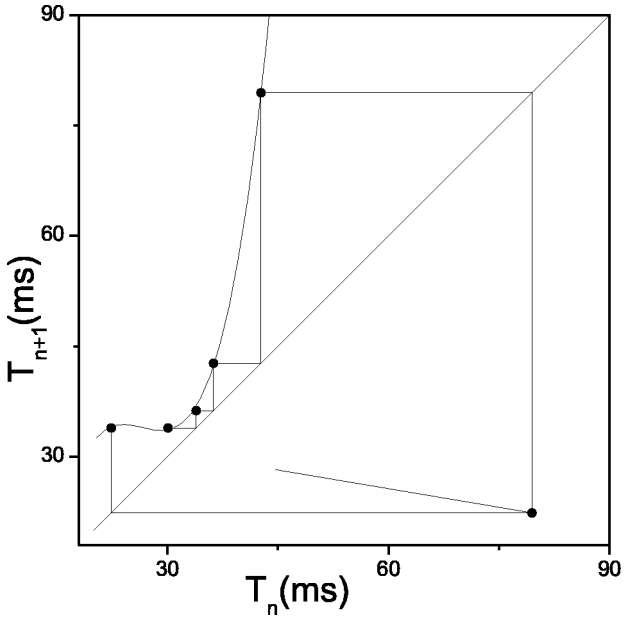

FIG. 12. Reconstructed attractor and a fitting to these experimental data.

from some fine-tuning of the coefficients of the piecewise map shown in Eq. (3).

In order to obtain an increasing sequence of period-adding bifurcations, we chose the following values for the control parameter μ: 0.0705 (period 4) in Fig. 13(a), 0.052 (period 5) in Fig. 13(b), 0.0447 (period 6) in Fig. 13(c), and 0.0415 (period 7) in Fig. 13(d). This sequence of control parameter values decreases the space between the cubic and the identity function, increasing the number of iterations through this corridor. The contact between the cubic function and the identity function indicates the critical point of a saddle-node bifurcation. In the bubbling system this point corresponds to a bubble growth starting from a positive bubble diameter, after the neck collapse, with the attractor point associated with this new bubbling mode, while the repeller point could be associated with liquid inflow through the nozzle.

In Fig. 14 are shown bubble profiles for some periodic bubbling of attractors shown in Fig. 11. In Fig. 14(a) the bubble pair shows an example of the periodic dynamics of period 2 observed in the attractor of Fig. 11(a), in which the first bubble distorts from an initially spherical shape to a flattened ellipsoidal shape. The wake of this bubble is a low-pressure region that penetrates the following bubble, bringing them into contact. In Fig. 14(b) is shown the bubbling in period 3 of the attractor of Fig. 11(b), a bubble pair followed by a single bubble. An image from period 4 is shown in Fig. 14(c), and despite the fact that there are three bubbles in the train, the large bubble at the top of the figure was formed by the coalescence of the two first bubbles. Close to the nozzle we can observe two bubbles before the coalescence for the next bubble cluster. In Fig. 14(d) is shown a period 5 with the same effect of coalescence for the first two bubbles, and finally the period 1 in Fig. 14(e) with the bubbles equally spaced.

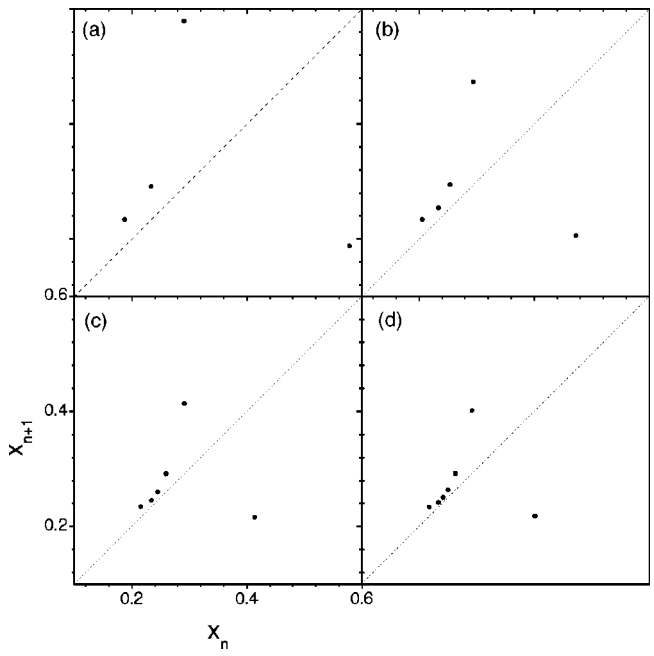

FIG. 13. Reconstructed attractors from the piecewise cubic map. The values of μ are (a) 0.0705, (b) 0.052, (c) 0.0447, and (d) 0.0415.

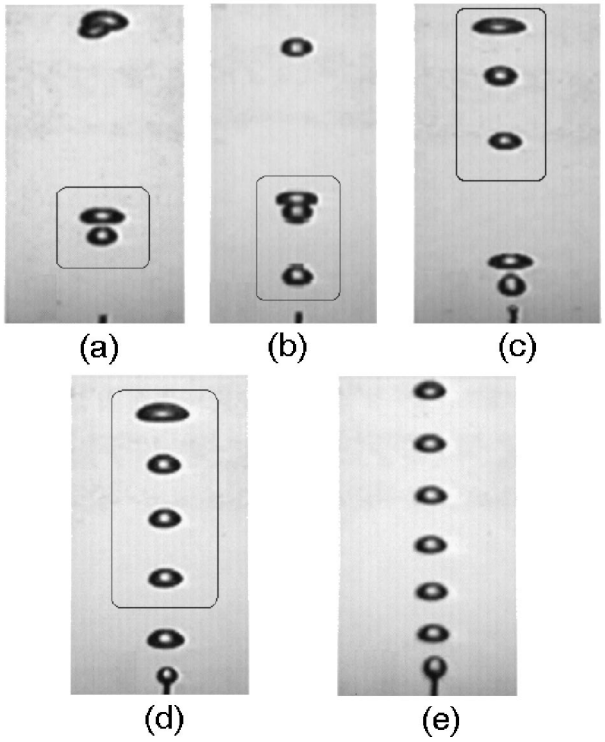

FIG. 14. Bubbles images for different bubbling regimes using the tube D, in which it is possible to observe period-adding phenomenon, (a)–(d), followed by a bubbling in a period 1 in (e). The boxes contain the elements of each bubble chain.

VI. CONCLUSIONS

We obtained the appearance of period-adding bifurcations in a bubble formation experiment using the air flow rate as the control parameter. Creation and destruction of orbits coexist in these bifurcations, obtained from the data of time interval between bubbles characterizing a bifurcation bubble. A geometrical parameter of the pneumatic system, the tube length, is used in order to vary the number of bifurcations. As one increased the tube length, more period-adding bifurcations were observed.

By means of image analyses, it is possible to arrive at a better understanding of the relationship between each dynamic state and the respective bubbling regime. There are two main types of bubble growth related to flow rate fluctuations inside the chamber under the nozzle for different bubbling regimes. In one type, during the bubble evolution there is a remarkable stage of bubble contraction, and in the other type the bubble grows continuously from a small bubble, created by the remaining air cone of the neck of the previous bubble. For some tube lengths, the interplay between these two bubbling modes for different flow rates generates periodic and chaotic behavior. Furthermore, each periodic bubbling of a period-adding sequence generates bubble trains, with observation of coalescence of the two first bubbles of a train for periods higher than three.

We studied the properties of piecewise nonlinear maps obtained from the experimental reconstructed attractors, observing the typical relaminarization process exhibited in period-adding bifurcations. As the control parameter is varied, a saddle-node bifurcation occurs, emulating the bubbling returning to a period 1.

The extended spatially system can be summarized as the follows: a pneumatic system with an excitation given by the singularity of bubble detachment. The pneumatic system is composed of the air reservoir, tubes, control system, chamber, and nozzle, which include many types of nonlinearity, such as pressure-flow characteristic in tubes and nozzles. Self-excited oscillations generated in systems by a steady air flow are very common, and examples can be found in the mechanism of phonation, or in some wind instruments, which are made to sound by blowing air across some sort of opening. From this point of view, a train of bubbles is a manifestation of a self-excited oscillation by blowing air through a submerged nozzle. The necking event and subsequent bubble detachment create a finite excitation, leading to a traveling pressure wave inside the pneumatic system. Hence, the tube length is an element of a selective amplifier of the excitation given by the bubble detachment. As a result, we observe period-adding bifurcation and chaos by placing different tubes, and using the air flow as the control parameter.

ACKNOWLEDGMENTS

This work is supported by the Brazilian agencies CNPq and FAPESP. The authors thank Hugo L. D. de S. Cavalcante for helpful discussions, and G. Liger-Belair for giving some information on the subject of bubbling regimes in carbonated beverages.

[1] A. Tufaile and J. C. Sartorelli, Phys. Rev. E **66**, 056204 (2002).
[2] D. Lohse, Phys. Today **55**, 36 (2002).
[3] L. Zhang and M. Shoji, Chem. Eng. Sci. **56**, 5371 (2001).
[4] G. Hernández-Cruz, H. Kantz, T. Letz, M. Ragwitz, E. Ramos, and R. Rechtman, Phys. Rev. E **67**, 036210 (2003).
[5] A. Tufaile and J. C. Sartorelli, Phys. Lett. A **287**, 74 (2001).
[6] A. Tufaile, M. B. Reyes, and J. C. Sartorelli, Physica A **308**, 15 (2002).
[7] K. Nguyen, C. S. Daw, M. Cheng, D. D. Bruns, C. E. A. Finney, and M. B. Kennel, Chem. Eng. J. **64**, 191 (1996).
[8] M. C. Ruzicka, Int. J. Multiphase Flow **26**, 1141 (2000).
[9] N. Acharya, M. Sem, and E. Ramos, Int. J. Heat Mass Transfer **46**, 1425 (2003).
[10] N. K. Kyriakides, E. G. Kastrinakis, S. G. Nychas, and A. Goulas, Can. J. Chem. Eng. **75**, 684 (1997).
[11] G. Liger-Belair, Ann. Phys. **27**, 1 (2002).
[12] Y. F. Huang, T. C. Yen, and J. L. Chern, Phys. Lett. A **199**, 70 (1995).
[13] W. Ren, S. J. Hu, B. J. Zhang, F. Z. Wang, Y. F. Gong, and J. X. Xu, Int. J. Bifurcation Chaos Appl. Sci. Eng. **7**, 1867 (1997).
[14] E. A. Jackson, in *Perspectives of Nonlinear Dynamics* (Cambridge University Press, Cambridge, 1995), Vol. 2, Chap. 5, p. 288.
[15] S. Coombes and A. H. Osbaldestin, Phys. Rev. E **62**, 4057 (2000).
[16] Y. Hasegawa, R. Tanaka, and Y. Ueda, Int. J. Bifurcation Chaos Appl. Sci. Eng. **11**, 3003 (2001).
[17] S. S. E. H. Elnashaie and A. Ajbar, Chaos, Solitons Fractals **7**, 1317 (1996).
[18] S. S. E. H. Elnashaie, H. M. Harraz, and M. E. Abashar, Chaos, Solitons Fractals **12**, 1761 (2001).
[19] G. Simon, P. Cvitanovic, M. T. Levinsen, I. Csabai, and A. Horvath, Nonlinearity **15**, 25 (2002).
[20] T. Nagatami, Phys. Rev. E **66**, 046103 (2002); Physica A **319**, 568 (2003).
[21] T. LoFaro, Math. Comput. Modell. **24**, 27 (1996).

[22] A. V. Holden and Y. Fan, Chaos, Solitons Fractals **2**, 221 (1992); **2**, 349 (1992).
[23] S. D. Brorson, D. Dewey, and P. S. Linsay, Phys. Rev. A **28**, 1201 (1983).
[24] E. Yellin and A. Rabinovitch, Phys. Rev. E **67**, 016202 (2003).
[25] V. Avrutin and M. Schanz, Chaos, Solitons Fractals **11**, 1949 (2000).
[26] S. U. Sarnobat, S. Rajput, D. D. Bruns, D. W. DePaolli, C. S. Daw, and K. Nguyen, Chem. Eng. Sci. **59**, 247 (2004).
[27] J. F. Davidson and B. O. G. Schüler, Trans. Inst. Chem. Eng. **38**, 335 (1960).